Ninth Canadian Conference on
Earthquake Engineering
Ottawa, Ontario, Canada
26-29 June 2007

FLANGE PARTICIPATION FOR SEISMIC DESIGN OF REINFORCED CONCRETE SHEAR WALLS

D. Palermo[1], A. Abdulridha[2], and M. Charette[3]

ABSTRACT

In the capacity design methodology, a flexural (ductile) shear wall is designed to promote inelasticity through formation of a plastic hinge at the base where the flexural demand is a maximum. This mechanism necessitates shear resistances corresponding to the development of the probable moment capacity of the wall system at its plastic hinge location. For rectangular-shaped shear walls, the evaluation of the moment capacity is a routine task; however, it is common in building construction to integrate L-, C-, T-, or H- shaped wall sections. For these section types the end flange walls participate in the moment capacity. Underestimating the effective flange width results in an underestimation of the probable moment capacity, which leads to design shear forces that are not necessarily conservative. A lower than required shear capacity would prevent the wall from developing a plastic hinge resulting in a shear-dominate failure mechanism with restricted ductility.

North American standards for reinforced concrete assume flange participation based on a percentage of the wall height. To asses the accuracy of current code requirements, a three-dimensional continuum finite element method is used to investigate the effectiveness of flange walls. Preliminary results from analyses indicate flange effectiveness in tension and compression can be larger than the current code prescribed values.

Introduction

Flanged sections are commonly considered in the design of lateral shear wall resisting systems, where part of the flange participates in the moment capacity of the section. However, in calculating the moment capacity, the effectiveness of the flange width requires attention to ensure a proper capacity design. Research has focused on the effectiveness of slabs built monolithically with supporting beams, highlighting the mechanism by which the slab participates in the lateral load resisting system of frame structures (Pantazopoulou and French 2001). Shear walls constructed with end flanges, on the other hand, have received little attention.

Code committees are conscious of the practical importance of the effective width concept, but they have struggled to specify what they perceive to be a conservative, yet fixed value that is suitable for a wide

[1]Assistant Professor, Dept. of Civil Engineering, University of Ottawa, Ottawa, Canada
[2]Doctoral Student, Dept. of Civil Engineering, University of Ottawa, Ottawa, Canada
[3]Research Assistant, Dept. of Civil Engineering, University of Ottawa, Ottawa, Canada

range of design conditions. The difficulty encountered in specifying a fixed width arises due to several influential parameters. Previous design standards for concrete, ACI 318-89 and CSA A23.3-94, recommended an effective flange overhang width of $h_w/10$, where h_w is the height of the wall above the section under consideration. This was based largely on results for T-beams, which is now considered to be a low value. Although a low effective width would underestimate flexural capacity, it is not necessarily conservative and could lead to inadequate shear reinforcement. Therefore, it was subsequently suggested that an effective flange overhang width of $h_w/4$ be implemented for the tension flange (Wallace 1996). The new provisions of ACI 318-05 and CSA A23.3-04 have incorporated this suggestion by stating that the effective width of overhanging flanges of structural walls shall not be assumed to extend farther from the face of the web than 25% of the total wall height above the section under consideration. Paulay and Priestley (1992) suggest an effective flange overhang of $50\%h_w$ and $15\%h_w$ for the tension and compression flange, respectively. The Structural Engineers Association of California implemented the Paulay and Priestley formulations in their Blue Book (SEAOC 1999).

Limited experimental work has been reported for structural walls constructed with flange overhangs exceeding the 25% effective flange width criteria specified by current standards. Barda (1976) tested eight low-rise flanged shear walls with height to length ratios ranging from 1:4 to 1:1, and flange overhang to height ratio from 0.133 to 0.533. The Nuclear Power Engineering Corporation of Japan (NUPEC 1995) conducted an experimental investigation of two large-scale flanged shear walls with flange overhang to height ratio of 0.72. The walls were subjected to dynamic loading conditions using a high-performance shaking table. Palermo and Vecchio (2002) implemented a test program involving two large-scale wide-flanged squat shear walls patterned after the type tested by NUPEC. Specimens DP1 and DP2, two originally undamaged specimens, were subjected to quasi-static reversed cyclic loading.

Research Significance

An accurate assessment of the effective flange width can be significant and of practical importance in the design or analysis of shear walls. For slender walls, underestimating the effective flange width leads to an underestimated moment capacity resulting in a shear-dominant mechanism rather than flexural yielding. Further, it underestimates the compression demand for the compression flange. In squat walls, the same conclusion can be stated for designs based on plane section theory. In designs based on the strut and tie methodology, evaluation of the effective flange width is necessary to determine the effective reinforcement in the tension tie and the effective concrete in the compressive strut.

This paper provides preliminary results of three-dimensional (3-D) non linear finite element analysis (NLFEA) of flanged shear walls. The nonlinear distribution of stresses along the flanges are evaluated through analysis and used to establish the effective flange width.

Finite Element Modeling and Verification

Analyses were undertaken using program VecTor3, a 3-D nonlinear finite element program (Vecchio and Selby 1991) incorporating the constitutive relationships and conceptual models of the Modified Compression Field Theory (Vecchio and Collins 1986). The program is applicable to 3-D solid concrete structures and assumes rotating, smeared cracks. The algorithm is based on a secant stiffness formulation using a total-load, iterative procedure. The reinforcement is typically modeled as smeared within the element but can also be discretely represented by truss bar elements. VecTor3 employs an 8-noded (24 degree of freedom) brick element which assumes linear displacement fields. As well, a 6-noded wedge element is available.

Wall DP1 (Palermo and Vecchio 2002) was selected for verification of the analysis procedure. DP1, a large-scale squat wide-flanged shear wall, was constructed with stiff top and bottom slabs. The top slab (4415 x 4000 x 640 mm) served to distribute the horizontal and axial loads to the walls of the structure. The bottom slab (4415 x 4000 x 620 mm), clamped to the laboratory strong floor, simulated a rigid foundation. The slabs were reinforced with No. 30 deformed reinforcing bars at a spacing of 350 mm in

each direction, with a top and bottom layer. The web wall, 2885 mm in length, 2020 mm in height, and 75 mm in thickness, was reinforced with D6 reinforcing bars. The bars were spaced 140 mm horizontally and 130 mm vertically in two curtains. The two flange walls were approximately 3045 mm long, 2020 mm high, and 95 mm thick. The flanges were also reinforced with D6 reinforcing bars, spaced 140 mm horizontally. The bars were spaced vertically at 130 mm near the web wall and 355 mm near the tips of the flanges. Dimensional details of DP1 are shown in Fig. 1 and material properties are listed in Table 1.

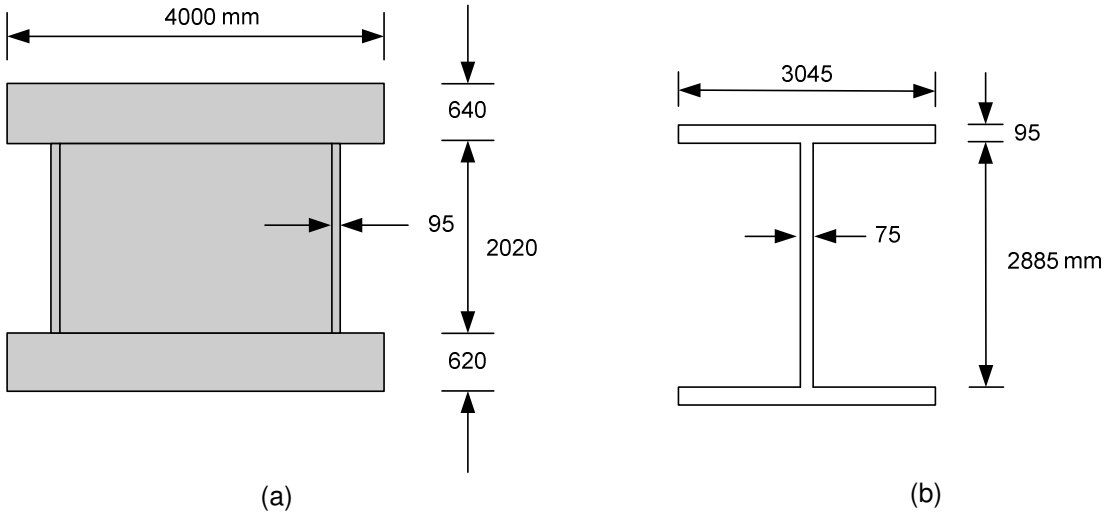

Figure 1. Details of Wall DP1: (a) dimensional details; (b) sectional details.

Table 1. Material Properties for Wall DP1.

Specimen	Zone	Concrete	Reinforcement			
			Horizontal		Vertical	
		f'_c (MPa)	ρ (%)	f_y (MPa)	ρ (%)	f_y (MPa)
DP1	Web	21.7	0.74	605	0.79	605
	Boundary	21.7	0.58	605	0.63/0.23*	605

*Footnote: Represents reinforcement near flange tips

Using symmetry, one-half of the structure was modeled using the mesh shown in Fig. 2. A total of 1026 8-noded brick elements were used, requiring 1892 nodes. The structure was assumed fully restrained at the base. The total vertical load, having a constant value of 600 kN for the half-model, was uniformly distributed among the interior nodes of the top slab. Loading was imposed on the top slab and involved horizontal displacements in increments of 1 mm until failure. The application of the loading was intended to simulate rigid diaphragm action of the top slab, which is common practice in seismic design.

The experimental and simulated results of the lateral load versus the horizontal displacement of the top slab are shown in Fig. 3. The observed and calculated responses are typical of shear-dominant behaviour. The analysis estimated a capacity of 1330 kN at a displacement of 12.5 mm, whereas a strength of 1298 kN corresponding to a displacement of 11.14 mm was reported during testing. The analysis predicted a failure mechanism involving shear crushing of the concrete, and the reinforcement in the flanges remained elastic. The predicted failure mode was consistent with the observed behaviour. A slight discrepancy is apparent in the post-peak region near ultimate load. This is a result of analysis conducted under monotonic loading in comparison to the reverse cyclic loading imposed during the experiment. Therefore, the softening of the concrete due to load cycling is not captured.

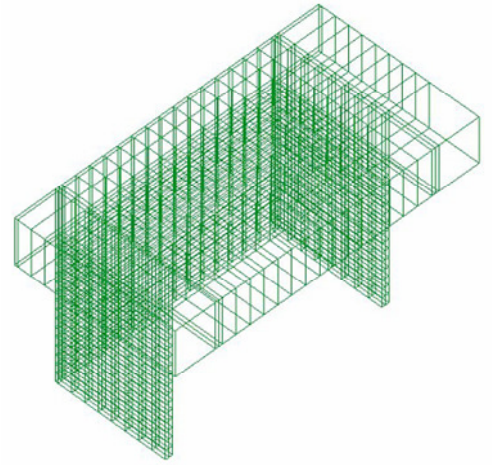

Figure 2. Finite Element Mesh for DP1.

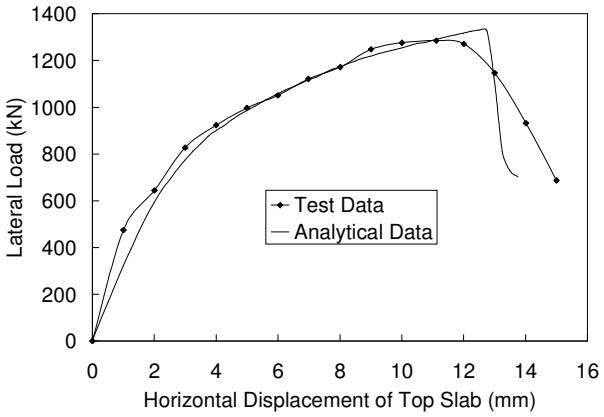

Figure 3. Load–Deformation Response of DP1.

Analysis Procedure

Flanged shear walls were analyzed using VecTor3 to investigate the variation of the effective flange width in squat and slender walls. The effective flange width was calculated using an approach similar to Hassan and El-Tawil (2003); represented by the following formulation:

$$b_{eff} = \frac{\sum_{i=1}^{n} \sigma_i w_i}{\sigma_{\max}} \tag{1}$$

Where σ_i average steel or concrete stress in element i for the tension and compression flange, respectively, w_i = width of element i, and $\sigma_{\max}$ = tensile or compressive stress at web-flange intersection for the tension and compression flange, respectively. The stresses are computed at the first layer of elements near the base of the wall. The effective flange overhang width as a function of the wall height was evaluated as:

$$\frac{b_{overhang}}{h_w} = \frac{b_{eff} - b_w/2}{h_w} \tag{2}$$

Where $b_{overhang}$ = the effective flange overhang width and b_w = the width of the web. Note that only half the web was included in the analysis due to modeling based on symmetry.

Analysis of Squat Walls

Barda (1976) tested a series of walls to investigate the shear stress of low-rise shear walls. Wall B1-1, which had a flange overhang width to wall height ratio of 0.267, was selected to demonstrate the flange effectiveness trends. Similar results were obtained for the other walls tested in this series. The horizontal length of the test wall was 1905 mm and the thickness was 102 mm. Boundary elements 610 mm wide and 102 mm thick were constructed at the extremities of the wall. These elements simulated cross walls or columns and contained flexural reinforcement. The wall was capped with a slab 1500 mm wide and 150 mm thick simulating a floor or roof element. A large base simulating a heavy footing was prestressed to the laboratory floor. Fig.4 illustrates the dimensional details of Wall B1-1 and the material properties are listed in Table 2.

The lateral load was applied to the wall through the top slab to a deflection of 75 mm. The mesh was divided into three zones, representing the web portion, the flanges, and the top slab. For analysis purposes, the bottom slab was omitted and the wall was assumed fully fixed at the base. The top slab was modeled as a stiff element through which loading was transferred to the wall section. Loading, consisting of predetermined lateral displacements, was imposed along the top slab in increments of 0.25 mm.

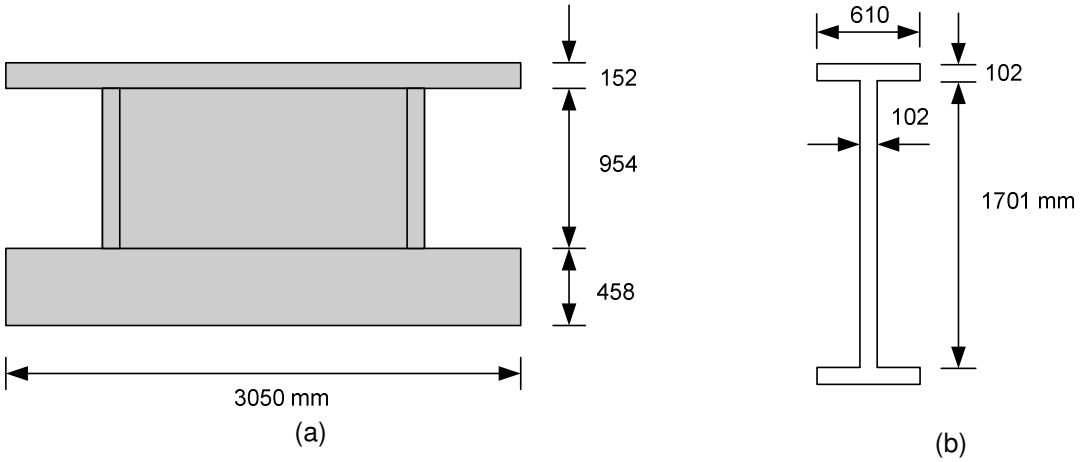

Figure 4. Details of Wall B1-1: (a) dimensional details; (b) sectional details.

Table 2. Material Properties of Wall B1-1.

Specimen	Zone	Concrete	Reinforcement			
			Horizontal		Vertical	
		f'_c (MPa)	ρ (%)	f_y (MPa)	ρ (%)	f_y (MPa)
B1-1	Web	30	0.5	414	0.5	414
	Boundary	30	0.5	414	1.8	414

The observed and calculated load-deformation responses for Wall B1-1 are shown in Fig. 5. A shear-dominant mechanism is captured by the analysis, and the calculated lateral resistance is similar to that observed. A load of 1203 kN was calculated at 5.5 mm of lateral displacement, compared with an observed capacity of 1217 kN at 5 mm.

The variation of vertical stresses in the tension and compression flanges is shown in Figs. 6 and 7, respectively. For the tension flange the average tensile stresses in the reinforcement are plotted, whereas for the compression flange, the average compressive stresses in concrete are shown. The resistance of the reinforcement after cracking of the concrete is the main contribution for the flange in tension and for the flange in compression, the concrete provides the main contribution to the capacity.

The shear lag effect is not severe for wall B1-1, indicating that the flange walls are highly effective at early stages of loading. The effective overhang width for the tension and compression flange for increasing drift ratio is shown in Figs. 8 and 9, respectively. For comparison, the A23.3-04 and Paulay and Priestley (1992) recommendations, along with the constructed flange overhang width are included. For the tension flange, the Paulay and Priestley model is limited by the actual flange overhang. The tension flange results indicate that the effectiveness is predicted sufficiently by A23.3-04 and Paulay and Priestley. For compression, the Paulay and Priestly model underestimates the effectiveness. Note that the effectiveness is constant with increasing drift since Eq. 1 calculates the effectiveness as a function of the stress at the web-flange intersection. Substituting σ_{max} with the yield stress of the vertical reinforcement for the flange in tension, and the cylinder compressive strength for the flange in compression would result in an increasing effectiveness with increasing drift.

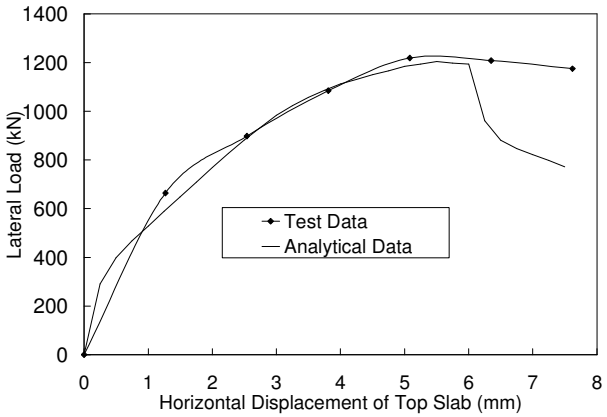

Figure 5. Load–Deformation Response of Wall B1-1.

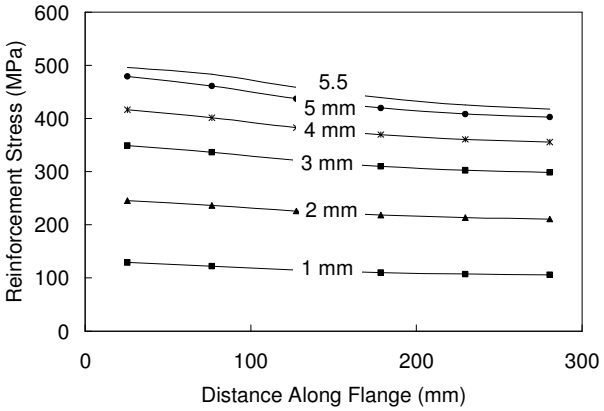

Figure 6. Stresses in Tension Flange.

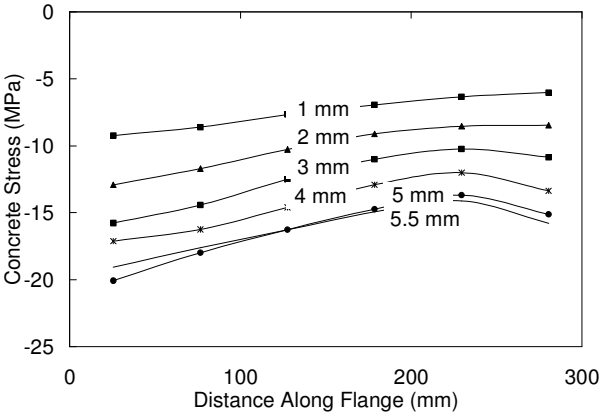

Figure 7. Stresses in Compression Flange.

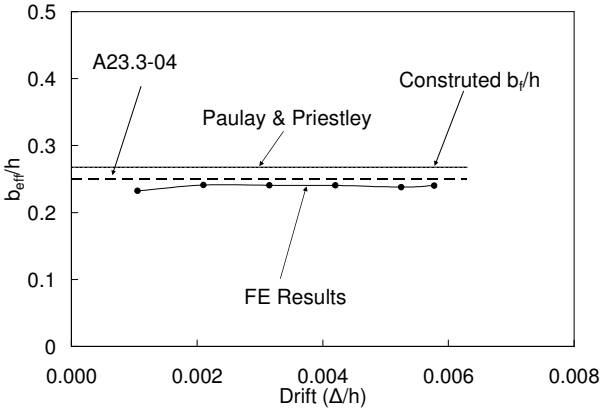

Figure 8. Effective Flange Width in Tension.

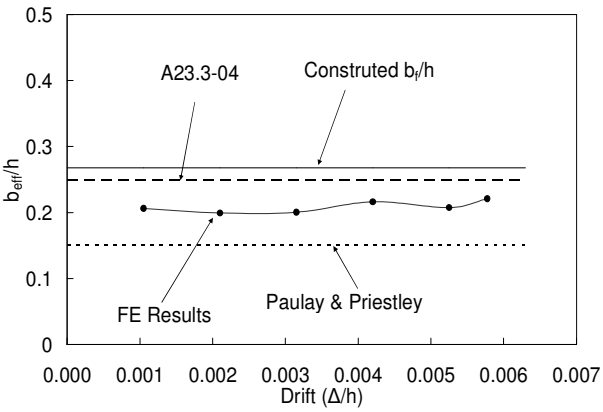

Figure 9. Effective Flange Width in Compression.

To investigate the upper limits on flange effectiveness, three additional models with similar material properties to B1-1, but with flange overhang width to wall height of 50%, 75% and 100% were analyzed. Figs. 10 and 11 demonstrate the flange overhang effectiveness for tension and compression, respectively. The maximum permissible flange effectiveness as predicted by A23.3-04 and Paulay and Priestley are also shown. No limit is imposed based on the actual flange overhang. The results indicate that the flange effectiveness increases as the flange widens and can exceed the values suggested by A23.3-04 and Paulay and Priestley. No upper limit is evident from the finite element results.

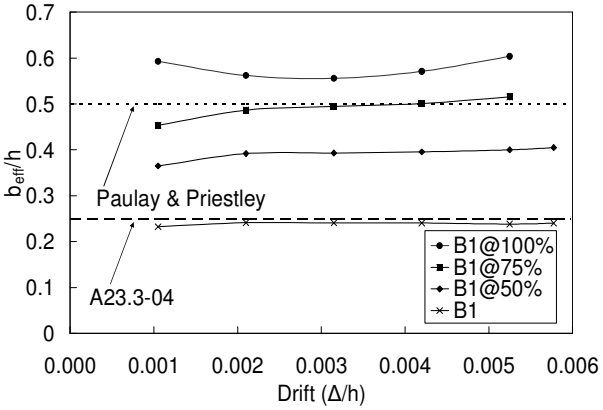

Figure 10. Effective Flange Width in Tension.

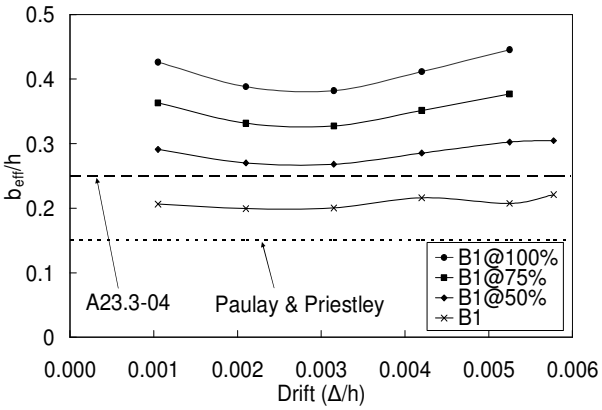

Figure 11. Effective Flange Width in Compression.

Results for Wall DP1 and DP2 tested by Palermo and Vecchio (2002) and U1 tested by NUPEC (1995) are shown in Figs. 12 and 13 for the computed effective overhang width in the tension and compression flanges, respectively. The walls were constructed with similar geometric properties and had flange overhangs to wall height of 73.5% and 71.9% for DP1 and DP2, and NUPEC, respectively. DP1 and U1 had similar axial load; however, the concrete strength in U1 was greater, allowing the reinforcement in the tension flange to yield prior to experiencing a shear crushing failure in the web wall. DP1 failed due to shear crushing without experiencing yielding of the flexural reinforcement. DP2 was similar to DP1, however, there was no applied axial load for DP2. The data indicates that the effective flanges generally exceed those specified by A23.3-04 and Paulay and Priestley. The initial larger flange effectiveness for the early stages of loading is a result of larger stresses at distances away from the web-flange intersection. Note that U1 demonstrates a flat response in tension, due to full yielding of the flexural reinforcement in the tension flange. Further, DP2 indicates a smaller effective flange in compression as a result of reduced axial load.

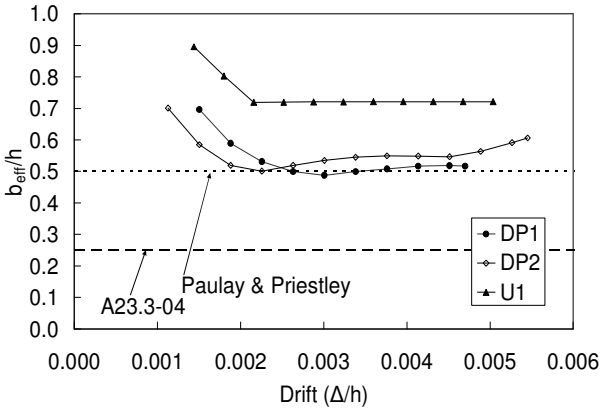

Figure 12. Effective Flange Width in Tension.

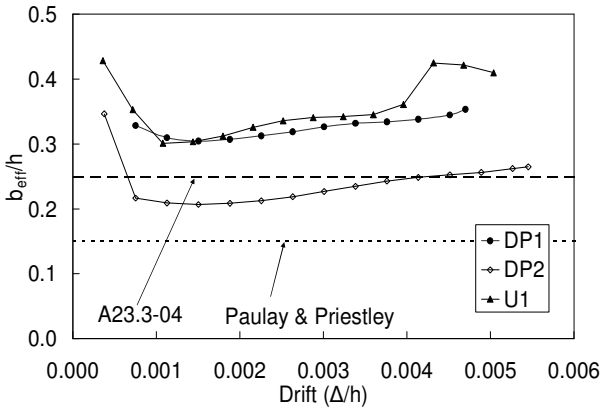

Figure 13. Effective Flange Width in Compression.

Analysis of Slender Walls

The series of walls tested by the Portland Cement Association (Oesterle et al. 1979), consisting of 1/3-scale representations of a five-story wall were selected for the investigation of flange effectiveness in slender walls. The series consisted of rectangular, barbell and flanged wall sections, measuring 1910 mm in total length and 4570 mm in height. Wall F2 was selected for analysis. The web wall was 102 mm thick and the flange width was 915 mm. The wall was built integral with a heavy base slab and stiff top slab. Wall F2 exhibited significantly yielding of the flexural and vertical web reinforcement in the flange and web, respectively, indicating that the response was dominated by flexural mechanisms prior to failure. Fig. 14 illustrates the details of Wall F2, and the material properties are listed in Table 3.

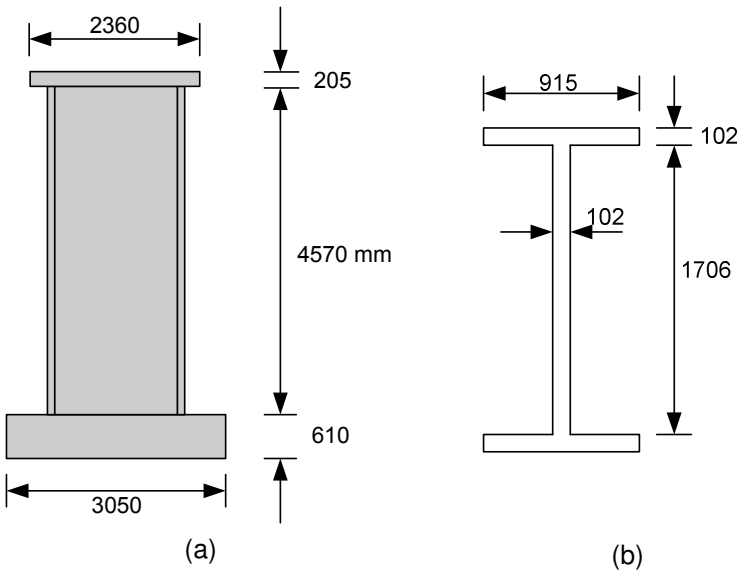

Figure 14. Details of Wall F2: (a) dimensional details; (b) sectional details.

Table 3. Material Properties of Wall F2.

Specimen	Zone	Concrete	Reinforcement			
			Horizontal		Vertical	
		f'_c (MPa)	ρ (%)	f_y (MPa)	ρ (%)	f_y (MPa)
F2	Web	45.6	0.63	430	0.31	430
	Boundary	45.6	0.63	430	4.35	430

The finite element mesh was divided into five zones: two to represent the web wall, two to model the flanges, one for the top slab. The wall was assumed fully fixed at the base, and the base slab was omitted. Loading, consisting of predetermined lateral displacements, was imposed along the stiff top slab in increments of 4 mm. The observed and calculated load-deformation responses for Wall F2 are shown in Fig. 15. The observed response indicates less load carrying capacity, due, in large part, to the effects of load cycling which was not captured in the monotonic analysis. Four additional models with the same material properties as F2 but with flange overhang width to wall height of 25%, 50%, 75%, and 100% were analyzed. The effect of flange overhang width to wall height is shown in Figs. 16 and 17, respectively for the tension and compression flange.

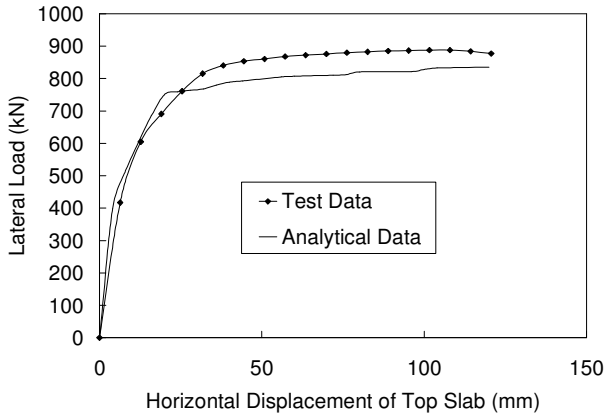

Figure 15. Load–Deformation Response of Wall F2.

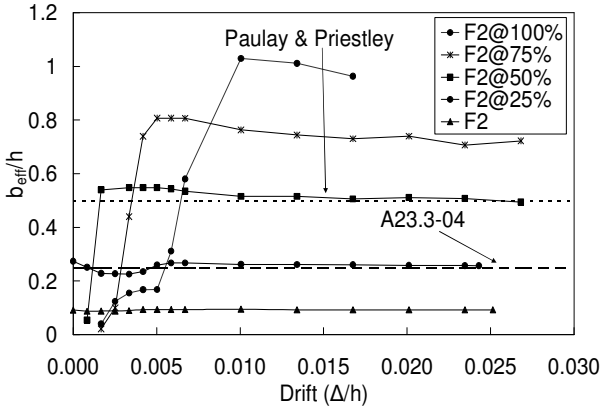

Figure 16. Effective Flange Width in Tension.

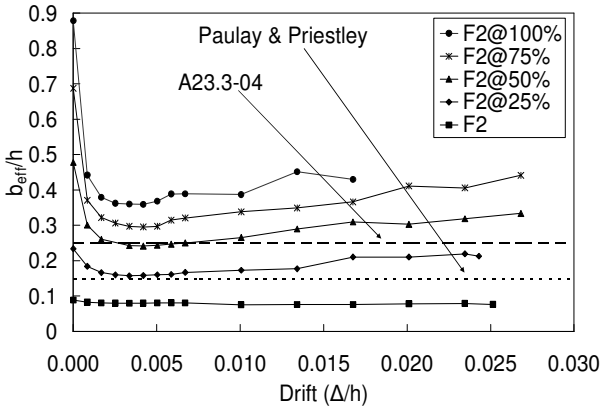

Figure 17. Effective Flange Width in Compression.

Similar to the response of the squat walls, the flange effectiveness in tension and compression for the slender wall indicates increasing flange overhang effectiveness as the actual flange widens, and the specified values of A23.3-04 and Paulay and Priestley can be exceeded. The initial larger flange effectiveness for the compression flange arises due to imposed axial loading present at the onset of loading.

Discussion of Results

The analysis of Walls B1-1, DP1, DP2, U1, and F2 demonstrates that the effective flange overhang width can exceed code prescribed values. These results are based on finite element results in which the base of the wall is assumed fully fixed, suggesting that the foundation has the capacity to develop the calculated flange overhang width. It appears that a larger than code imposed effective flange can be assumed provided the foundation has the strength to sustain the moment developed from the assumed flange effective width. Further, the effectiveness of flanges in tension is larger than flanges in compression, which is similar to the findings of Paulay and Priestley. Although the tension flange may be more critical for strength calculations, an incorrect effective flange width in compression has implications on the required buckling and or confinement reinforcement, stability and rotation capacity of walls. Underestimating the compression flange effectiveness will result in a larger compression zone, resulting in a reduced rotation capacity.

The preliminary investigation presented herein suggests that additional analyses are warranted to determine more realistic values of flange effectiveness such that the flange overhang width is not underestimated. Parameters such as axial load, wall height to length ratio, and influence of drift when the overhang is estimated as a function of yield stress of reinforcement for the flange in tension and cylinder compressive strength for the flange in compression. Further the effects of load cycling which could lead to redistribution of stresses should be addressed through 3-D reverse cyclic load analysis.

Conclusions

A preliminary study using three-dimensional nonlinear finite elements has been conducted on flanged shear walls to investigate the effectiveness of overhanging flanges. Based on limited analyses the following observations are suggested:

1. Three-dimensional nonlinear continuum finite elements can successfully simulate the response of flanged walls.
2. The effectiveness of flanges in tension and compression increase with increasing flange width and no upper limit has been found.
3. The effectiveness of flanges in tension is larger than flanges in compression.
4. No significant trend is evident between flange effectiveness and drift for flange effectiveness evaluated as a function of the stress at the web-flange intersection.
5. The CSA A23.3-04 specifications generally underestimates the effective flange in tension as the actual

overhang exceeds 25% of the wall height. For flanges in compression the A23.3-04 generally underestimates the effectiveness when the actual overhang width exceeds 50% of the wall height.
6. The Paulay and Priestley formulation for effective tension flanges is exceeded when the actual flange overhang exceeds 75% of the wall height or walls with overhangs exceeding 50% of the wall height that experience full yielding of the tensile reinforcement along the flange.
7. The Paulay and Priestley formulation for effective compression flanges is exceeded in all cases, unless the actual flange overhang width is less than the 15% effective width limit.

References

American Concrete Institute, 1989. *Building Code Requirements for Structural Concrete and Commentary*, Farmington Hills.

American Concrete Institute, 2005. *Building Code Requirements for Structural Concrete and Commentary*, Farmington Hills.

Barda, F., Hanson, J. M., and W. G. Corley, 1976. Shear Strength of Low-Rise Walls with Boundary Elements, *Bulletin RD043.01D*, Portland Cement Association, Detroit.

Canadian Standards Association, 1994. *Design of Concrete Structures*, Rexdale.

Canadian Standards Association, 2004. *Design of Concrete Structures*, Mississauga.

Hassan, M., and S. El-Tawil, 2003. Tension Flange Effective Width in Reinforced Concrete Shear Walls, *ACI Structural Journal,* 100 (3), 349-356.

Nuclear Power Engineering Corporation of Japan, 1996. Seismic Shear Wall ISP: NUPECs Seismic Ultimate Dynamic Response Test, *Report OCED/GD (96) 188*, Organization for Economic Co-Operation and Development, Paris.

Oesterle, R.G., Aristizabal-Ochoa, J. D., Fiorato, A. E., Russell, H. G., and Corley, W. G., 1979. Earthquake Resistant Structural Walls, Tests of Isolated Walls, Phase II, *Report No. PB80132418*, Portland Cement Association, Skokie.

Palermo, D., and F. J. Vecchio, 2002. Behavior of Three-Dimensional Reinforced Concrete Shear Walls, *ACI Structural Journal,* 99 (1) 81-89.

Pantazopoulou, S. J., and C. W. French, 2001. Slab Participation in Practical Earthquake Design of Reinforced Concrete Frames, *ACI Structural Journal* 98 (4), 479-489.

Paulay, T., and Priestley, M. J. N., 1992. *Seismic Design of Reinforced Concrete and Masonry Buildings*, John Wiley and Sons, Inc., New York, NY.

Structural Engineers Association of California, 1999. *Recommended Lateral Force Requirements and Commentary*, Sacramento.

Vecchio, F. J., and Selby, R. G., 1991. Toward Compression-Field Analysis of Reinforced Concrete Solids, *ASCE Journal of Structural Engineering*, 117 (6), 1740-1758.

Vecchio, F. J., and Collins, M. P., 1986. The Modified Compression-Field Theory for Reinforced Concrete Elements Subjected to Shear, *ACI Structural Journal* 83 (2), 219-231.

Wallace, J. W., 1996. Evaluation of UBC-94 Provisions for Seismic Design of RC Structural Walls, *Earthquake Spectra* 12 (2), 327-348.